Research Article
doi.org/10.1002/cmdc.202200091
Chemistry Europe
European Chemical Societies Publishing

www.chemmedchem.org

Evaluation of a Radiolabeled Macrocyclic Peptide as Potential PET Imaging Probe for PD–L1

Nedra Jouini,[a, b, c] Jens Cardinale,[a, c] and Thomas L. Mindt*[a, b, c]

The interaction between the immune checkpoint PD-1 and PD–L1 promotes T-cell deactivation and cancer proliferation. Therefore, immune checkpoint inhibition therapy, which relies on prior assessment of the target, has been widely used for many cancers. As a non-invasive molecular imaging tool, radiotracers bring novel information on the *in vivo* expression of biomarkers (e.g., PD–L1), enabling a personalized treatment of patients. Our work aimed at the development of a PD–L1-specific, peptide-based PET radiotracer. We synthesized and evaluated a radiolabeled macrocyclic peptide adapted from a patent by Bristol Myers Squibb. Synthesis of [^{68}Ga]Ga-NJMP1 yielded a product with a radiochemical purity > 95 % that was evaluated *in vitro*. However, experiments on CHO–K1 hPD–L1 cells showed very low cell binding and internalization rates of [^{68}Ga]Ga-NJMP1 in comparison to a control radiopeptide (WL12). Non-radioactive cellular assays using time-resolved fluorescence energy transfer confirmed the low affinity of the reported parent peptide and the DOTA-derivatives towards PD–L1. The results of our studies indicate that the macrocyclic peptide scaffold reported in the patent literature is not suitable for radiotracer development due to insufficient affinity towards PD–L1 and that C-terminal modifications of the macrocyclic peptide interfere with important ligand/receptor interactions.

Introduction

The inhibitory immune checkpoint Programmed cell Death receptor 1 (PD-1) and its ligand Programmed cell Death Ligand 1 (PD–L1) is widely researched since its discovery in the early nineties.[1] The interaction between PD-1 and PD–L1 inhibits T-cell signaling, therefore rendering the immune system ineffective for fighting diseases. PD-1 (CD 279) is a membrane receptor critical for the regulation of adaptive immune cells such as T-lymphocytes.[2] PD–L1 (CD274) is a transmembrane protein that is expressed on immune-related lymphocytes and overexpressed by cancer cells, thus, allowing for their efficient evasion from the host immune system. To activate the immune system, the inhibition of the interaction between PD-1 and PD–L1 can be achieved on either target and is now a clinical option for immune-oncology therapies.[3] To date, several well-established compounds for immune checkpoint inhibition (ICI) therapy have been developed, such as antibodies like Atezolizumab (targeting PD–L1) and Nivolumab (targeting PD-1).[4] Early reports on the different therapeutic antibodies that successfully received approval by the Food and Drug Administration (FDA) demonstrated the efficacy of PD-1/PD–L1 inhibition therapy in different types of cancers including non-small cell lung carcinoma (NSCLC) and melanoma.[5] To benefit from an immune checkpoint blockade therapy, the expression of the target (e.g., PD–L1) should be evaluated beforehand. The most frequently applied method for this is immunohistochemistry (IHC) staining of formalin-fixed, paraffin-embedded biopsy samples. However, there is considerable variability in the used techniques: differences in the binding sites of the used anti-PD–L1 staining antibodies, the choice of the staining method (automatic versus manual), and the technical protocols are all factors that give rise to incomparable results. The absence of a standardized method for staining and scoring of PD–L1 leads to an incomplete picture of the heterogeneously expressed target.[6] The non-invasive molecular imaging modality Positron Emission Tomography (PET) offers a promising alternative to the current IHC for detecting the PD–L1 expression and therefore predicting the response to immunotherapy treatment.[7–8] ImmunoPET, which employs antibody-based PET radiotracers for the imaging of immune checkpoints, has witnessed an increased usage over the past years.[9] However, radiolabeled antibodies can present unfavorable characteristics such as low tissue penetration, costly production, slow pharmacokinetics and thus, longer diagnosis time (days to weeks). Smaller molecules with faster pharmacokinetics that are able to target protein-protein interactions, in this case PD-1/PD–L1, have recently gained attention in the field of radiopharmaceutical development.[10] In comparison to bulkier PD–L1 inhibitors (e.g., antibodies and other proteins), synthetically readily accessible peptides exhibit several advantages such as excellent specificity, low toxicity, good tissue penetration,

[a] MSc. N. Jouini, Dr. J. Cardinale, Prof. Dr. T. L. Mindt
Ludwig Boltzmann Institute Applied Diagnostics
General Hospital of Vienna
Währinger Gürtel 18–20, 1090 Vienna (Austria)
E-mail: thomas.mindt@univie.ac.at
[b] MSc. N. Jouini, Prof. Dr. T. L. Mindt
Faculty of Chemistry, University of Vienna
Währinger Strasse 42, 1090 Vienna (Austria)
[c] MSc. N. Jouini, Dr. J. Cardinale, Prof. Dr. T. L. Mindt
Division of Nuclear Medicine, Medical University of Vienna
Währinger Gürtel 18–20, 1090 Vienna (Austria)

Supporting information for this article is available on the WWW under https://doi.org/10.1002/cmdc.202200091

fast pharmacokinetics, and low production costs. All these features make peptides promising candidates for the development of PD–L1 imaging probes.[11–13] Our study focused on the synthesis, characterization and evaluation of a novel peptide-based radiotracer which targets PD–L1. The 14-mer macrocyclic peptide (BMS78), adapted from a library of peptides published in a patent by Bristol Myers Squibb (BMS),[14] was equipped with the universal chelator 2,2′,2″,2‴-(1,4,7,10-tetraazacyclo-dodecane-1,4,7,10-tetrayl)tetraacetic acid (DOTA) at its C-terminus for ^{68}Ga-labelling (**NJMP1**) and the conjugate was evaluated *in vitro* using the Chinese Hamster Ovary cell line expressing human PD–L1 (CHO–K1 hPD–L1). The reported and established radiolabeled PD–L1-targeting macrocyclic peptide WL12 was used as a reference compound.

Results and Discussion

Selection of the PD–L1 targeting peptide

Protein-protein interactions (PPI) have been shown to play a vital role in regulating biological processes within the co-stimulatory and inhibitory immune checkpoints. However, targeting PPIs with small molecules presents its own challenges since the PD-1/PD–L1 interaction surface is quite large (1,97 Å^2) and featureless.[15] In the past years, BMS published multiple patents disclosing structures of immunomodulatory macrocyclic peptides that inhibit the interaction between PD-1 and PD–L1. The corresponding *in vitro* data was also disclosed, revealing several promising compounds with reportedly high affinities towards the target protein PD–L1.[16] Research conducted by other teams based on structures included in these patents have narrowed down the library to a couple of potential macrocyclic peptides with 13 to 15 amino acid sequences, able to inhibit the PD-1/PD–L1 interaction.[17] The X-ray analysis of two of these peptides (BMS71 and BMS57) bound to PD–L1 have meanwhile been published, providing resourceful information in determining our choice of peptides for the development of a PD–L1 radiotracer.[17] Based on the available information at the onset of our studies, BMS71 was chosen because of its reported low IC_{50} value (7 nM) and different favorable interactions of its amino acid residues with PD–L1. Beforehand, we reviewed the published co-crystal structure of BMS71/PD–L1 (Protein Data Bank (PDB) ID: 5O45; see Supporting Information (SI) Figure S13) where the C-terminal amino acid amide (Gly^{14}-NH_2) was reported to point away from the PPI interface and not to form important interactions with the receptor PD–L1. Thus, it appeared that the C-terminus offers an easily accessible conjugation site for the modification of the peptide with chelators for radiometal labelling.[17] Although, as discussed below, this notion had to be revised at a later time point after new structural data became available.[18]

The well-established macrocyclic peptide WL12 was equipped with the chelator DOTAGA, radiolabeled with [^{68}Ga]$GaCl_3$ and used as a reference PD–L1 radiotracer for *in vitro* assays. WL12 is a PD–L1 targeting peptide that has been demonstrated to bind with high affinity to PD–L1 (IC_{50} = 23 nM).[13,19] It is among the first macrocyclic peptides that has shown promising *in vitro* and *in vivo* results after being radiolabeled with various radionuclides (copper-64, gallium-68 and fluorine-18).[13,19,20] Currently, WL12 is being investigated in clinical trials as a PD–L1 targeting PET-tracer in gastrointestinal and lung cancer (*NCT04304066*[21]). [^{64}Cu]Cu-WL12 has also been recently used as a quantifying tool for target engagement of therapeutic anti-PD–L1 antibodies, improving therefore the therapeutic doses applied to the patients in clinics.[22] Manual Fmoc-Solid Phase Peptide Synthesis (SPPS) was used to synthesize the linear 14/15-amino acid sequence of BMS71, BMS78, and NJMP1 (Table 1, SI Figure S10).

Synthesis of macrocyclic peptides and their derivatives

After the first attempts to synthesize BMS71, we observed an instability in the *N*-methyl amide rich peptide sequence (^{m}Phe^2-^{m}Nle^3-^{m}Gly^4). It has been reported that for peptides containing several consecutive *N*-methylated amino acids, fragmentation during the trifluoroacetic acid-mediated cleavage from the resin can occur at the N-terminal positions.[23–25] This made the synthesis of BMS71 by standard SPPS very challenging. The low yields of the synthesis of BMS71 (approx. 5 %) and the difficult separation of multiple side products prompted us to choose another sequence, BMS78. The latter is only one-amino acid different from the first peptide (Gly^4 instead of ^{m}Gly^4) and it was reported to show a good binding affinity towards PD–L1 in the published BMS patent (IC_{50} = 14 nM).[14]

With an *N*-methyl amide less, it could be assumed that BMS78 is not prone to degradation during standard SPPS. Indeed, the synthesis of BMS78 and NJMP1 (Table 1, Figure 1) on a Rink amide resin proceeded without problems. For NJMP1, the synthesis started with the coupling of the Fmoc-Lys(DOTA(O*t*Bu)$_3$)-OH to the resin in order to place the chelator at the C-terminal amino acid of the peptide. Even though the coupling of Fmoc-Lys(DOTA)–OH to the resin has been reported to be challenging due to steric reasons, the reaction proceeded smoothly in our hands.[26] Once the linear sequences were

Table 1. Amino acid sequences of investigated peptides and peptide conjugates and corresponding yields.

Peptide	Sequences[a]	Yields	Purity (HPLC)
BMS71	Cyclo(AcPhe–^{m}Phe–^{m}Nle–^{m}Gly–Asp–Val–^{m}Phe–Tyr–^{m}Gly–Trp–Tyr–Leu–Cys)-Gly–NH_2	5 %	83 %
BMS78	Cyclo(AcPhe–^{m}Phe–^{m}Nle–Gly–Asp–Val–^{m}Phe–Tyr–^{m}Gly–Trp–Tyr–Leu–Cys)-Gly–NH_2	50 %	98 %
NJMP1	Cyclo(AcPhe–^{m}Phe–^{m}Nle–Gly–Asp–Val–^{m}Phe–Tyr–^{m}Gly–Trp–Tyr–Leu–Cys)-Gly–Lys(DOTA)-NH_2	42 %	98 %
WL12	Cyclo(AcTyr–^{m}Ala–Asn–Pro–His–Leu–Hyp–Trp–Ser–Trp(Me)-^{m}Nle–^{m}Nle–Orn(DOTAGA)-Cys)-Gly–NH_2	68 %	97 %

[a] The thioether bridge is located between Cys^{13} and Ac–Phe^1 for NJMP1, BMS71, BMS78, and between Cys^{14} and Ac–Tyr^1 for WL12.

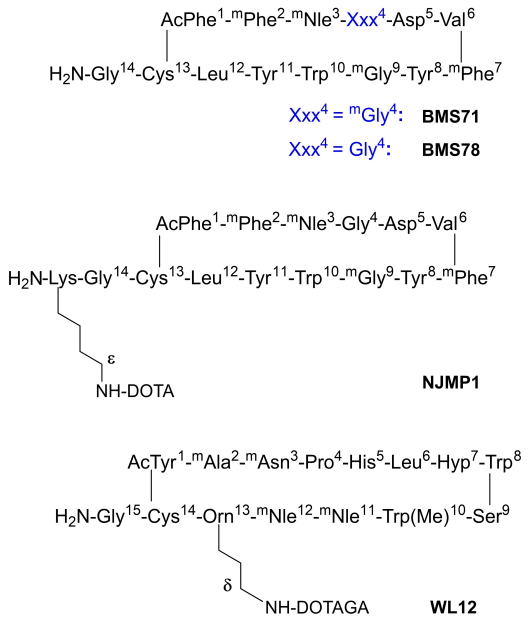

Figure 1. Structures of the peptides and peptide-conjugates investigated in this work.

elongated, chloroacetic acid was coupled to the last amino acid (Phe[1]). The peptides were then cleaved from the resin and deprotected, and the cyclization between the thiol group of Cys[13] and the chloroacetylated Phe[1] was carried out.[17] Both compounds BMS78 and NJMP1 were obtained in higher yields than BMS71 (Table 1) and in excellent purities. Electrospray Ionization Mass Spectrometry (ESI-MS) of the HPLC-purified compounds confirmed their structures (SI Table S1, Figures S1, S2 and S3). The conjugation of 2,2′,2″-(10-(2,6-dioxotetrahydro-2H-pyran-3-yl)-1,4,7,10-tetraazacyclododecane-1,4,7-triyl)triacetic acid (DOTAGA-anhydride) to Orn[13] of the commercial WL12 peptide was conducted according to a published procedure.[13] The crude product was purified by Reverse Phase (RP)–HPLC and the structure of the conjugate was confirmed by ESI-MS (Table S1, Figure S6).

^{nat}Ga- and ^{68}Ga-labelling of NJMP1 and WL12

Metalation reactions of NJMP1 and WL12 with $^{nat}Ga(NO_3)_3$ and [^{68}Ga]$GaCl_3$ were performed according to literature procedures yielding the desired products in quantitative yields and high purities (>95%).[27–28] ^{nat}Ga-NJMP1 and ^{nat}Ga-WL12 were purified by RP-HPLC, lyophilized, and analysis by ESI-MS confirmed their structures (SI Table S1 and Figures S4, S7). [^{68}Ga]Ga-NJMP1 and [^{68}Ga]Ga-WL12 were prepared with a radiochemical purity (RCP) and radiochemical yield (RCY) of >95% (SI Figures S5 and S8).

$LogD_{pH\ 7.4}$ and human serum stability assay

The lipophilicity of a radiolabeled compound is an important indicator for potential unspecific binding to non-targeted tissues. $LogD_{pH7.4}$ of [^{68}Ga]Ga-NJMP1 and [^{68}Ga]Ga-WL12 were determined using the Shake-flask method (n=3 in triplicate) and are given as mean values±standard deviation (SD).[29–30] [^{68}Ga]Ga-NJMP1 displayed a $LogD_{pH\ 7.4}$ of 0.795±0.22 indicating a rather lipophilic character of the compound. For [^{68}Ga]Ga-WL12, a calculated value of LogP=−5.99 has been reported.[13] Our shake-flask experiments showed that [^{68}Ga]Ga-WL12 is less hydrophilic with a $LogD_{pH\ 7.4}$ of −1.22±0.23. This value falls in the range of the reported $LogD_{pH\ 7.4}$ for [^{64}Cu]Cu-NOTA-WL12 (−0.818±0.026) demonstrating the hydrophilicity of the radiolabeled peptide.[31] Overall, WL12 presents more charged amino acids in its cyclic structure than NJMP1 (Figure 1) and thus, the observed differences in $LogD_{pH\ 7.4}$ were to be expected.

The stability of [^{68}Ga]Ga-NJMP1 was evaluated in human serum at 37 °C. [^{68}Ga]Ga-NJMP1 was stable in serum after 2 h (>93% as determined by γ-HPLC; Figure S14). As the results of the lipophilic character of NJMP1, a substantial amount of radioactivity was found associated with the protein pellet (approx. >50% after 90 min).

Receptor binding and cell internalization assays

Receptor binding and cell internalization assays were performed with CHO–K1 hPD–L1 and CHO–K1 as a negative control. The CHO–K1 hPD–L1 cell line was passaged fewer than ten times in order to avoid a decrease in the efficiency of the hPD–L1 transfection while maintaining reliable results.[32] To our surprise, the receptor binding and uptake of [^{68}Ga]Ga-NJMP1 in the CHO–K1 hPD–L1 cell line was <2% AD (applied dose)/10^6 cells after 90 min (Figure 2, Table 2). Cell binding and uptake of [^{68}Ga]Ga-NJMP1 in CHO–K1 cell line was negligible. The time point t=90 min was chosen as a reference point after initial cell experiments with [^{68}Ga]Ga-NJMP1 during which the cell binding and internalization rates did not change after two hours (SI Figure S11).

Various cell lines have been used for the *in vitro* evaluation of PD–L1 radiotracers. Despite the lack of a standardized method and a commonly used PD–L1-expressing cell line, we decided to validate our own set-up for the evaluation of NJMP1. We therefore performed the same cell binding and internalization assays with [^{68}Ga]Ga-WL12 (Figure 2, Table 2, SI Fig-

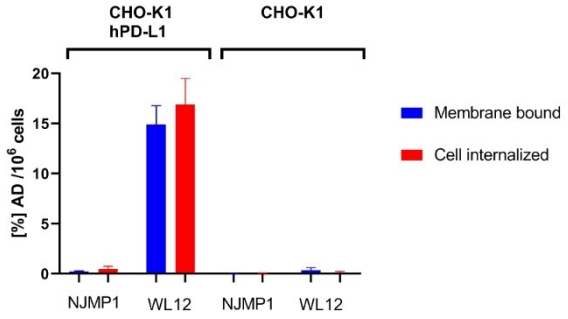

Figure 2. A comparison of receptor binding and cell internalization between [^{68}Ga]Ga-NJMP1 and [^{68}Ga]Ga-WL12 on CHO–K1 hPD–L1 and CHO–K1 cells at 90 min. Data are presented as mean values±SD (n=3 in triplicate).

Table 2. Membrane bound and cell internalized fractions in CHO–K1 and CHO–K1 hPD–L1 cell line for [68Ga]Ga-WL12 and [68Ga]Ga-NJMP1 after 90 min. Data are presented as mean values ± SD (n = 3 in triplicate).

Cell line		[^{68}Ga]Ga-NJMP1	[^{68}Ga]Ga-WL12
CHO–K1 hPD–L1	Membrane bound %AD/10^6 cells	0.36 ± 0.06	18.17 ± 1.75
	Cell internalization %AD/10^6 cells	1.68 ± 0.19	19.18 ± 1.6
CHO–K1 (negative control)	Membrane bound %AD/10^6 cells	0.133 ± 0.01	3.5 ± 0.30
	Cell internalization %AD/10^6 cells	1.18 ± 0.04	3.07 ± 0.43

ure S12). Each approx. 18% AD/10^6 cells were found membrane bound and internalized, respectively, in the CHO–K1 hPD–L1 cells after 90 min indicating a high affinity of [^{68}Ga]Ga-WL12 towards PD–L1. Experiments with [^{68}Ga]Ga-WL12 and the PD–L1 negative control cell line CHO–K1 resulted in a reduced cell binding and internalization of each approx. < 4% AD/10^6 cells, therefore demonstrating the specificity of [^{68}Ga]Ga-WL12 towards PD–L1. For complete *in vitro* data of [^{68}Ga]Ga-WL12 including results of blocking experiments see the SI, Figure S12. We were able to generate good and reproducible *in vitro* results for the binding and internalization of [^{68}Ga]Ga-WL12 to PD–L1 as well as provide proof of its specificity to the target in accordance with published data.[20,33]

The CHO–K1 and CHO–K1 hPD–L1 cell lines that constituted the used *in vitro* test system were therefore validated and the unfavourable low binding and internalization of [^{68}Ga]Ga-NJMP1 could only be on account of the intrinsic characteristics of the parent peptide BMS78 and/or the structural modifications that were introduced. The lack of binding of [^{68}Ga]Ga-NJMP1 to PD–L1 *in vitro* led us to resort to non-radioactive assays for quantitative measurement of the affinity (IC_{50}) of BMS78 and its derivatives towards PD–L1 as well as to test the extent of the loss of affinity that could be ascribed to its C-terminal modification with DOTA. For this purpose, we used the homogenous time-resolved fluorescence PD-1/PD–L1 biochemical binding assay (HTRF). This method is comparable to the one utilized by BMS,[14] although the specific assay conditions were not fully disclosed in the patents. We first measured the IC_{50} of known PD–L1 blockers such as Atezolizumab (IC_{50} = 2.25 nM) and Inhibitor 3^{TM}, a commercially available PD–L1 inhibiting peptide (IC_{50} = 186 nM). The measured IC_{50} of both compounds were in good agreement with literature values (Table 3, Figure 3A).[34–35] However, the IC_{50} value for BMS78 was found an order of magnitude higher than what was reported in the

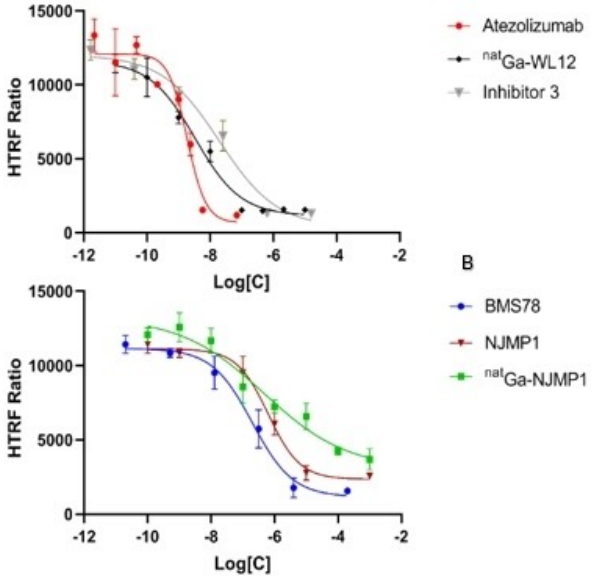

Figure 3. PD-1/PD–L1 blockade HTRF bioassay. A) Concentration-dependent inhibition curves for Atezolizumab, inhibitor 3^{TM} and ^{nat}Ga-WL12, which were used as reference compounds for this assay. B) Concentration-dependent inhibition curves for BMS78, NJMP1, and ^{nat}Ga-NJMP1. Data are presented as mean values ± SD (n = 2–3 in triplicate).

patent (Table 3, Figure 3B).[14] Similarly, another report on PD–L1-targeting macrocyclic BMS peptides (e.g., BMS57) also discloses lower binding affinities towards PD–L1 than those presented in the BMS patents.[36] C-terminal modified NJMP1 and ^{nat}Ga-NJMP1 displayed even higher values than BMS78, with an increase of the IC_{50} from the nM to the μM range. While the attachment of Lys(DOTA)NH_2 to the C-terminus of BMS78 resulted in a doubling of the IC_{50} compared to BMS78, loading the chelator with ^{nat}Ga had even a bigger impact and further increased the IC_{50} by two orders of magnitude. We can currently not provide an explanation for this phenomenon. However, the (positive or negative) impact of radiometalation as well as the influence of different radiometals on the binding affinity of peptide-chelator conjugates towards their respective molecular targets has previously been reported.[37–39] Although the co-crystal structure of BMS71/PD–L1 indicated a C-terminal Gly^{14}-NH_2 that was pointing away from the main hydrophobic binding site of PD–L1 (SI Figure S13),[17] our results suggest that the modification in this position could have either altered the binding mechanism of the peptide or, alternatively, interfered with important ligand-receptor interactions.

Table 3. IC_{50} values measured by the Homogenous Time resolved Fluorescence (HTRF) PD-1/PD–L1 assay. Data are presented as mean values ± SD (n = 2–3 in triplicate).

Compound	Measured IC_{50} [nM]	95% CI [nM]	Reported IC_{50} [nM]
Atezolizumab	2.25 ± 0.36	1.292–7.667	3.83[35]
BMS78	133 ± 1.23	106.3–166.9	14[14]
NJMP1	242 ± 0.89	218.2–278.7	–
^{nat}Ga-NJMP1	25945 ± 1450	15320–54990	–
^{nat}Ga-WL12	12.41 ± 0.25	10.09–16.08	^{nat}Cu-WL12 = 2.3[13]
Inhibitor 3^{TM}	186 ± 1.69	165.1–209.5	146[35]

With the substantial decrease in PD–L1 affinity from BMS78 (IC_{50} 133 nM) to NJMP1 (IC_{50} 242 nM) and ^{nat}Ga-NJMP1 (IC_{50} 26 μM), the observed lack of binding of [^{68}Ga]Ga-NJMP1 to CHO–K1 hPD–L1 cells became obvious. Thus, our hypothesis that the modification of the C-terminal amino acid of BMS78 (Gly^{14}) negatively impacts the overall binding of NJMP1 to PD–L1 could be confirmed.

In the course of our investigations, Zhong et al. reported a pharmacophore mapping study with the macrocyclic peptide BMS71 which complements our observations.[18,40] The interaction of BMS71/PD–L1 is driven by major hydrophobic interactions between the non-polar amino acids of the peptide (e.g., Phe^1, $^mNle^3$, Val^6) and the "hot spots" of PD–L1.[41] However, few polar interactions and hydrogen bonds were also found to be important, especially since hydrogen bonds from the backbone amides contribute to the stabilization of the cyclic structure of the peptide. Few of the amino acid residues found within the PD–L1 "hot-spots" (e.g., Glu^{58}) were shown to form important hydrogen bonds with the C-terminal Gly^{14}-NH_2 of BMS71 (and therefore BMS78). By attaching a Lys(DOTA)NH_2 to the Gly^{14} of BMS78, we have likely interfered with some important polar interactions and, in addition, added more steric bulk. All these factors in turn impacted the binding of the peptide-conjugate NJMP1 to PD–L1. It might be possible to improve the PD–L1 binding properties of radiolabeled derivatives of BMS71/BMS78 (e.g., by choosing a different site for DOTA conjugation), however, the currently limited binding affinity of the parent macrocyclic peptides renders them unsuitable lead structures for the development of PD–L1 targeting PET radiopharmaceuticals.

Experimental Section

Unless stated otherwise, all reagents and solvents were purchased from Iris Biotech (Marktredwitz, Germany), and Merck (Darmstadt, Germany) and used without further purification. Fmoc-amino acids, *N*-methylated Fmoc-amino acids, Rink Amide MBHA LL resin (100–200 mesh), N,N-diisopropylcarbodiimide (DIC) and ethyl cyano(hydroxyimino)acetate (OXYMA Pure) were purchased from Merck Biosciences (Nottingham, UK) or Iris Biotech (Marktredwitz, Germany). Solid Phase Peptide Synthesis (SPPS) was performed manually. Fmoc-Lys(DOTA(O*t*Bu)$_3$)-OH was purchased from Macrocyclics (Texas, USA). Polypropylene syringes fitted with polypropylene frits and a polypropylene plunger were obtained from Multi-Syntech (Witten, Germany) and teflon taps from Biotage (Uppsala, Sweden). PD–L1 inhibitor 3™, a commercially available macrocyclic peptide targeting PD–L1 used for the validation of the HTRF assay, was purchased from SelleckChem (Texas, USA). WL12, a macrocyclic peptide used as a reference compound for *in vitro* experiments (structure shown in SI Figure S9) was purchased from BioVision (California, USA). Atezolizumab was purchased from Evidentic GmbH (Berlin, Germany). The Human PD1/PD–L1 biochemical binding assay HTRF was purchased from Cisbio Perkin Elmer (Massachusetts, USA). HPLC analysis was carried out with an Agilent system (Vienna, Austria) equipped with Autosampler Agilent 1100 Series, Iso Pump Agilent 1200 Series G1310 A, UV-Monitor Agilent 1200 Series G1314B Variable Wavelength Detector (VWD) and Radioactivity Detector Elysia Raytest Gabi Star. Data acquisition and gradient control were performed using GINA Star™, version 5.9. HTRF assay read-outs were performed on a Molecular Devices FlexStation 3 Multi-mode micro-plate reader (San José, USA). The γ-counter used in this work was a 2480 Wizard2, PerkinElmer (Waltham, USA). The Centrifuge was a Hettich Universal 30 RF with Hettich rotor 1412 24×3 g/24×1,5–2,2 mL (Tuttlingen, Germany). Data and statistical analysis were carried with GraphPad Prism5 ®. Low resolution (LR)–Mass Spectrometry (MS) was performed on a Bruker maXis (UHR-TOF, Vienna, Austria) equipped with Electrospray ionization (ESI) ion source and 3D ion trap and High resolution (HR)–MS was recorded on a Bruker maXis UHR-TOF spectrometer. HPLC solvents were 0.1% trifluoroacetic acid (TFA) in H_2O (A) and acetonitrile (MeCN) (B). Semi-preparative separation of the peptide derivatives was performed using Chromolith® SemiPrep RP-18 endcapped column (100–10 mm), followed by analytical HPLC on the Chromolith® Performance RP-18 endcapped column (100–4.6 mm) and a linear gradient from 70% to 30% of eluent (A) in 13 min (20 min for BMS71), flow rate 0.6 mL/min. Quality control of the radiolabeled peptides was performed using a Chromolith® Performance RP-18 endcapped column (100–4.6 mm) and a linear gradient from 70% to 30% of eluent (A) in 13 min with a flow rate of 0.6 mL/min.

Peptide synthesis of BMS71 and BMS78

BMS71 and BMS78[14] both comprise a common cyclic 14-mer amino acid sequence with one amino acid difference (Sar^4 versus Gly^4) as shown in Table 1 and in Figure 1. The resin (Rink Amide MBHA LL, 0.015 mmol) was swollen in 3 mL of N, N-dimethylformamide (DMF) in a syringe fitted with a polypropylene frit and a teflon tap. Standard coupling procedure (a) consisted of adding the Fmoc-protected amino acid (0.06 mmol, 4.0 equiv.), OXYMA Pure (0.06 mmol, 4.0 equiv.) and DIC (0.06 mmol, 4.0 equiv.), mixed in 1 mL of DMF to the resin, and the suspension was shaken for 15 min at 75 °C. Double coupling procedures (b) were used for *N*-methylated amino acids; the *N*-methyl-Fmoc-protected amino acid (0.06 mmol, 4.0 equiv.), OXYMA Pure (0.06 mmol, 4.0 equiv.) and DIC (0.06 mmol, 4.0 equiv.) mixed in 1 mL of DMF, were added to the resin, and the suspension was shaken for 15 min at 75 °C. The solvent was removed by filtration, and the resin was washed three times with 3 mL of DMF and 3 mL of dichloromethane (CH_2Cl_2). Then the second coupling was performed by the same procedure. After the second coupling, the reaction mixture was left shaking for 6 hours at room temperature (RT). The solvent was removed by filtration, and the resin was washed three times with 3 mL of DMF and 3 mL of CH_2Cl_2. Completion of the reaction was monitored by Kaiser Test or *n*-Chloranil Test (for secondary amines). For Fmoc deprotection, 20% piperidine in 3 mL DMF was added to the resin and left to react for 3 min at RT. The deprotection agent was then filtered off, and this process was repeated three times. The resin was then washed three times with 3 mL of DMF and 3 mL CH_2Cl_2. The yield of the deprotection was determined by UV measurement ($\lambda = 301$ nm) of the fluorenylmethylpiperidine adduct ($\varepsilon = 7800\ mol^{-1}\ dm^3\ cm^{-1}$). After completion of the elongation of the amino acid sequence, and before cleaving the peptide from the resin, chloroacetic acid (0.06 mmol, 4.0 equiv.) was coupled to the N-terminus using the standard amino acid coupling procedure (a). The peptide sequences were cleaved and deprotected by a treatment of 2 h with 2 mL of 90% TFA and 10% triisopropylsilane mixture that was afterward removed by evaporation with a stream of air. The crude peptides were then precipitated by the addition of ice-cold diethyl ether Et_2O (15 mL). After centrifugation (4000 rpm, 3×5 min, 4 °C) and two washing steps with cold Et_2O, the linear peptide sequences were used for the cyclization procedure as described below.

NJMP1 synthesis

NJMP1 (BMS78 C-terminally conjugated to Lys(DOTA)NH_2) was synthesized according to the following procedure. Fmoc-Lys(DOTA(O*t*Bu)$_3$)-OH (0.02 mmol, 1.0 equiv.) was added to OXYMA and DIC (each 0.06 mmol, 3.0 equiv.) in 1 mL of DMF, then coupled to the resin prior to the elongation of the peptide sequence according to the coupling procedure (a). The reaction mixture was reacted for 15 min at 75 °C and then left shaking overnight at RT. The completion of the reaction was monitored with a Kaiser test. Acetylation of the unreacted amines of the resin was performed with 2.5 mL of a mixture of 90% DMF, 5% DIPEA, 5% Ac_2O by agitating for 10 min at RT. The elongation of the sequence and final coupling of chloroacetic acid followed the procedures described above.

Cyclization procedure

1 mg of the crude linear peptides were dissolved in a (1:2, v/v) mixture of acetonitrile and aqueous ammonium bicarbonate buffer (0.1 M, pH 8.5, 24 mL) and the solution was afterwards left shaking overnight at RT. The reaction mixture was then concentrated and the obtained products were dissolved in 500 μL (1:1, v/v) of a mixture of acetonitrile/water and purified by RP-HPLC. The analytical HPLC of the cyclized BMS71 had a retention time of and $t_R = 9{,}13$ min. The cyclized peptides BMS78 and NJMP1 had a retention time of $t_R = 6{,}43$ min and $t_R = 6{,}33$ min, respectively. The obtained lyophilized peptides were characterized by ESI-MS.

Synthesis of WL12

4 mg (2 μmol, 1.0 equiv.) of WL12 peptide and DOTAGA-anhydride (10 μmol, 5.0 equiv.) were dissolved in 1 mL of DMF and N,N-diisopropylethylamine (DIPEA, 5.0 equiv.) was added to the mixture that was left shaking overnight at RT. After the completion of the reaction, DMF was removed *in vacuo* and the residue was dissolved in a mixture (1:1, v/v) of H_2O and MeCN for RP-HPLC purification. The analytical HPLC of WL12 resulted in a retention time of $t_R =$ 7,94 min. The obtained lyophilized compound was characterized by ESI-MS.

^{nat}Ga-labelling of peptide NJMP1 and WL12

The DOTAGA- and DOTA-conjugated peptides (0.08 μmol, 1.0 equiv.) were dissolved in 50 μL of HEPES buffer (pH = 3) and $Ga(NO_3)_3 \cdot 6H_2O$ (0.39 μmol, 5.0 equiv.) dissolved in 50 μL HEPES buffer was added. The mixtures were stirred for 30 min at 75 °C and afterwards purified with RP-HPLC. ^{nat}Ga-NJMP1 was collected at $t_R =$ 7,12 min and ^{nat}Ga-WL12 at $t_R = 8{,}2$ min with a purity of 98% for the final peptide conjugates. The obtained lyophilized peptides were characterized by ESI-MS and stored at 4 °C for later use.

^{68}Ga-labelling of peptide NJMP1 and WL12

A ^{68}Ge/^{68}Ga generator (IRE Elit Radiopharma) was eluted with approx. 1 mL of 0.1 M HCl yielding an eluate of approx. 1 mL (450 MBq). In the reaction mixture, we added the peptide precursors (1.7 nmol, 4 μL) from 1 mg/mL stock solutions prepared in a H_2O/MeCN mixture (1:1, v/v), to sodium acetate buffer (22 μL, 1 M, pH 4.5) and 44 μL of the eluted [^{68}Ga]$GaCl_3$. The mixture, with a final pH 4.3, was reacted for 13 min at 95 °C. Quality control of the obtained radiolabeled peptides ($A_s = 2.5$ MBq/μg) consisted of analytical radio-HPLC to check the radiochemical purity of the compound. The retention time for the [^{68}Ga]Ga-NJMP1 was $t_R =$ 7,4 min and $t_R = 8{,}7$ min for [^{68}Ga]Ga-WL12 (SI Figures S5, S8).

PD-1/PD–L1 biochemical binding assay

Cisbio (Perkin Elmer) provides a commercially available competitive inhibition assay, promoted to discover novel inhibitors for the immune checkpoint PD-1/PD–L1. The assay relies on time-resolved fluorescence resonance energy transfer (TR-FRET) and uses PD–L1-6His-tag and PD-1-Ig that can be detected by anti-human IgG-Eu^{3+} cryptate and anti-6HIS-XL665 monoclonal antibody, respectively. For the plating of the compounds, the instructions in the leaflet of the assay provided by the company were followed.

Cell lines

Chinese Hamster Ovary cell line CHO–K1 (CHO) were purchased from the American Type Culture Collection (ATCC, Manassas, VA), and passaged less than ten times before the experiments. CHO–K1 cells were maintained in Ham's F-12 medium with 10% Fetal Bovine Serum (FBS, Gibco) and 1% Penicillin/Streptomycin (P/S). Recombinant CHO–K1 cells stably expressing human PD–L1 (hPD–L1), henceforth referred to as CHO–K1 hPD–L1, were purchased from BPS Bioscience (San Diego, California) and were maintained in F-12 K medium with 10% FBS, 1% P/S, and 2 mg/mL G418. The cells were cultured in an incubator at 37 °C in an atmosphere containing 5% CO_2 and passaged less than ten times before seeding out for cell internalization experiments.

Cell internalization and receptor binding assay

Internalization studies were performed as previously published.[42,43] Briefly, approx. 10^6 CHO–K1 hPD–L1 or CHO–K1 cells were seeded in F-12 K medium containing 10% FBS, 1% P/S and 2 mg/mL G418 in 6-well plates on the day before the experiment and incubated overnight in a humidified incubator (37 °C, 5% CO_2). Approx. one hour before the experiment, the medium was replaced with 1.3 mL fresh 1% FBS F-12 K medium. Subsequently, 100 μL of the radiolabeled peptide [^{68}Ga]Ga-NJMP1 or [^{68}Ga]Ga-WL12 were added to each well (100 μL per well; 15 pmol; ~1.0 kBq) and cells were incubated for different time points (30, 60, 90 and 120 min). After the respective incubation times, the supernatant was collected and the cells were washed twice with 1 mL ice-cold Dulbecco's phosphate-buffered saline (PBS). The combined fractions represent the unbound radioligand. The receptor-bound radioactivity was obtained by incubating the cells twice for 5 min with an ice-cold acidic glycine solution (100 mM NaCl, 50 mM glycine, pH 2.8; 1 mL) on ice followed by the removal of the supernatant. Finally, the internalized fraction was collected after cell lysis using 1 M NaOH (1 mL; 10 min; 37 °C; 5% CO_2) and the wells containing the cell lysate were washed twice with NaOH (1 M, 1 mL). Standards of the radio-labeled peptides [^{68}Ga]Ga-NJMP1 and [^{68}Ga]Ga-WL12, for the determination of the applied dose, were prepared in triplicate. All fractions were measured in a γ-counter (409–613 keV energy window) and calculated as a percentage of the applied dose (AD) per one million cells.

$LogD_{pH7.4}$ determination

The lipophilicity (LogD) of [^{68}Ga]Ga-NJMP1 and [^{68}Ga]Ga-WL12 was determined by the partition coefficient between n-octanol and PBS (pH 7.4) utilizing the "shake-flask method".[28–29] PBS and n-octanol were shaken overnight to saturate each phase. After the separation of the layers by centrifugation at 4500 rpm for 5 min at 23 °C, equal volumes (500 μL) of each layer were taken and transferred into an Eppendorf tube and 5 μL (~5 kBq) of the radiolabeled peptide solutions (formulated in saline solution) were added to the PBS/n-octanol mixture. The resulting solutions were left shaking for

20 min, then centrifuged at 3000 rpm for 10 min. Aliquots of 300 μL were removed from the n-octanol and PBS phases and the radioactivity was measured in the γ-counter (n = 3 in triplicates). The lipophilicity was calculated as the LogD value of the average ratio between the radioactivity in the organic (n-octanol) and the PBS fractions.

Stability assay in human serum

For the determination of the serum stability, the radiopeptide [^{68}Ga]Ga-NJMP1 (100 μL; 15 pmol, 0.105 MBq) was added to 900 μL of fresh human blood serum and incubated (37 °C, 5 % CO_2). 100 μL of acetonitrile were dispensed into three tubes and at preselected time points (30, 60, and 90 min) samples of 100 μL serum were taken and added to the solvents in the tube to precipitate the proteins. The tube was thoroughly vortexed for 2 min at 5200 rpm, then 75 μL were taken from the supernatant and diluted with 75 μL of MilliQ Water. The mixture was then analyzed by γ-HPLC to determine the formation of potential metabolites. The protein pellet was washed 3 times with saline, centrifuged and measured in a gamma counter in order to quantify the protein-bound fraction of radioactivity.

Conclusion

In summary, we have synthesized and evaluated *in vitro* some $^{68/nat}$Ga-labeled peptide conjugates based on a macrocyclic scaffold described in patents of BMS. The radiolabeled [^{68}Ga]Ga-NJMP1 as well as ^{nat}Ga-NJMP1 were tested *in vitro* using cell binding experiments and HTRF screening assays and compared with the corresponding WL12 reference compounds. The results from our investigations indicate that the parent peptide BMS78 (lacking the chelator) has a much lower affinity towards PD–L1 than what was reported in the patent literature. In addition, C-terminal modification of the macrocyclic peptide with a DOTA chelator further decreased its affinity towards PD–L1 likely due to disturbance of important hydrogen bonding interactions with the receptor. On the other hand, the reference compound used in our studies, ^{68}Ga-labeled macrocyclic peptide WL12 with the chelator DOTAGA attached to an amino acid within the macrocycle (Orn^{13}), exhibited better properties. We also describe the first validation of a PD–L1 *in vitro* test system composed of CHO–K1 hPD–L1/CHO–K1 cells, which can be used in the future for the reliable evaluation of other PD–L1 targeted radiotracers. We conclude that the macrocyclic parent peptides BMS71 and BMS78 show potential in inhibiting the PD-1/PD–L1 interaction, but their low binding affinity towards PD–L1 makes them unsuitable lead structures for the development of PET radiotracers for the imaging of PD–L1.

Acknowledgements

We thank the Mass Spectrometry Service Centre of the University of Vienna, Dr. Barbara Lieder (Institute of Physiological Chemistry, University of Vienna) for help with the HTRF measurements, Dr. Marie Brandt, Anna Stingender, and Katarína Benčurová (Ludwig Boltzmann Institute Applied Diagnostics) as well as Dr. Verena Pichler and Karsten Bamminger (Department of Biomedical Imaging and Image-guided Therapy (Division of Nuclear Medicine) of the general hospital of Vienna) for their general and technical support. Open Access Funding was provided by the University of Vienna.

Conflict of Interest

The authors declare no conflict of interest.

Data Availability Statement

The data that support the findings of this study are available in the supplementary material of this article.

Keywords: radiopharmaceuticals · peptides · immune checkpoint blockade · PET · PD-1/PD–L1

[1] K. Bardhan, T. Anagnostou, V. A. Boussiotis, *Front. Immunol.* **2016**, *7*, 550.
[2] B. T. Fife, K. E. Pauken, *Ann. N. Y. Acad. Sci.* **2011**, *1217*, 45–59.
[3] L. Chen, X. Han, *J. Clin. Invest.* **2015**, *125*, 3384–3391.
[4] K. M. Hargadon, C. E. Johnson, C. J. Williams, *Int. Immunopharmacol.* **2018**, *62*, 29–39.
[5] Y. Jiang, M. Chen, H. Nie, Y. Yuan, *Hum. Vaccines Immunother.* **2019**, *15*, 1111–1122.
[6] X. Meng, Z. Huang, F. Teng, L. Xing, J. Yu, *Cancer Treat. Rev.* **2015**, *41*, 868–876.
[7] S. Nimmagadda, *Cancers (Basel)*. **2020**, *12*.
[8] F. Bensch, E. L. van der Veen, M. N. Lub-de Hooge, A. Jorritsma-Smit, R. Boellaard, I. C. Kok, S. F. Oosting, C. P. Schroder, T. J. N. Hiltermann, A. J. van der Wekken, H. J. M. Groen, T. C. Kwee, S. G. Elias, J. A. Gietema, S. S. Bohorquez, A. de Crespigny, S. P. Williams, C. Mancao, A. H. Brouwers, B. M. Fine, E. G. E. de Vries, *Nat. Med.* **2018**, *24*, 1852–1858.
[9] W. Wei, Z. T. Rosenkrans, J. Liu, G. Huang, Q. Y. Luo, W. Cai, *Chem. Rev.* **2020**, *120*, 3787–3851.
[10] M. Konstantinidou, T. Zarganes-Tzitzikas, K. Magiera-Mularz, T. A. Holak, A. Domling, *Angew. Chem. Int. Ed.* **2018**, *57*, 4840–4848; *Angew. Chem.* **2018**, *130*, 4932–4940.
[11] A. Signore, A. Annovazzi, M. Chianelli, F. Corsetti, C. Van de Wiele, R. N. Watherhouse, *Eur. J. Nucl. Med.* **2001**, *28*, 1555–1565.
[12] U. Hennrich, M. Benešová, *Pharmaceuticals* **2020**, *13*, 38.
[13] S. Chatterjee, W. G. Lesniak, M. S. Miller, A. Lisok, E. Sikorska, B. Wharram, D. Kumar, M. Gabrielson, M. G. Pomper, S. B. Gabelli, S. Nimmagadda, *Biochem. Biophys. Res. Commun.* **2017**, *483*, 258–263.
[14] M. M. Miller, C. Mapelli, M. P. Allen, M. S. Bowsher, E. P. Gillis, D. R. Langley, E. Mull, M. A. Poirier, N. Sanghvi, L.-Q. Sun, D. J. Tenney, K.-S. Yeung, J. Zhu, K. W. Gillman, Q. Zhao, K. A. Grant-Young, P. M. Scola (Bristol Myers Squibb), WO2016039749 A1, **2016**.
[15] K. M. Zak, R. Kitel, S. Przetocka, P. Golik, K. Guzik, B. Musielak, A. Domling, G. Dubin, T. A. Holak, *Structure* **2015**, *23*, 2341–2348.
[16] X. Lin, X. Lu, G. Luo, H. Xiang, *Eur. J. Med. Chem.* **2020**, *186*, 111876.
[17] K. Magiera-Mularz, L. Skalniak, K. M. Zak, B. Musielak, E. Rudzinska-Szostak, L. Berlicki, J. Kocik, P. Grudnik, D. Sala, T. Zarganes-Tzitzikas, S. Shaabani, A. Domling, G. Dubin, T. A. Holak, *Angew. Chem. Int. Ed.* **2017**, *56*, 13732–13735; *Angew. Chem.* **2017**, *129*, 13920–13923.
[18] Y. Zhong, X. Li, H. Yao, K. Lin, *Molecules* **2019**, *24*, 1940.
[19] W. G. Lesniak, R. C. Mease, S. Chatterjee, D. Kumar, A. Lisok, B. Wharram, V. R. Kalagadda, L. A. Emens, M. G. Pomper, S. Nimmagadda, *Mol. Imaging* **2019**, *18*, 1-9.
[20] R. A. De Silva, D. Kumar, A. Lisok, S. Chatterjee, B. Wharram, K. Venkateswara Rao, R. Mease, R. F. Dannals, M. G. Pomper, S. Nimmagadda, *Mol. Pharm.* **2018**, *15*, 3946–3952.

[21] H. Zhu, '' Research for the Molecular Imaging of the PD–L1 Targeting Tracer", can be found under https://clinicaltrials.gov/ct2/show/NCT04304066, **2020**.
[22] D. Kumar, A. Lisok, E. Dahmane, M. McCoy, S. Shelake, S. Chatterjee, V. Allaj, P. Sysa-Shah, B. Wharram, W. G. Lesniak, E. Tully, E. Gabrielson, E. M. Jaffee, J. T. Poirier, C. M. Rudin, J. V. Gobburu, M. G. Pomper, S. Nimmagadda, *J. Clin. Invest.* **2019**, *129*, 616–630.
[23] M. J. O. Anteunis, C. Auwera, *Int. J. Pept. Protein Res.* **2009**, *31*, 301–310.
[24] Y. Yang, in: *Side Reactions in Peptide Synthesis* (Ed.: Y. Yang), Academic Press, **2016**, pp. 1–31.
[25] M. Teixido, F. Albericio, E. Giralt, *J. Pept. Res.* **2005**, *65*, 153–166.
[26] M. W. Pennington, M. E. Byrnes, *Methods Mol. Biol.* **1994**, *35*, 1–16.
[27] M. A. Green, M. J. Welch, *Nuclear Medicine and Biology* **1989**, *16*, 435–448.
[28] D. Mueller, W. A. Breeman, I. Klette, M. Gottschaldt, A. Odparlik, M. Baehre, I. Tworowska, M. K. Schultz, *Nat. Protoc.* **2016**, *11*, 1057–1066.
[29] C. A. Fischer, S. Vomstein, T. L. Mindt, *Pharmaceuticals* **2014**, *7*, 662–675.
[30] C. Vraka, L. Nics, K. H. Wagner, M. Hacker, W. Wadsak, M. Mitterhauser, *Nucl. Med. Biol.* **2017**, *50*, 1–10.
[31] J. Jiang, D. Li, T. Liu, L. Xia, X. Guo, X. Meng, F. Liu, F. Wang, Z. Yang, H. Zhu, *Bioorg. Med. Chem. Lett.* **2021**, *40*, 127901.
[32] P. Hughes, D. Marshall, Y. Reid, H. Parkes, C. Gelber, *BioTechniques* **2007**, *43*, 575–586..
[33] H. Z. A. Z. Y. Jiang Jinquan, *J. Nucl. Med.* **2020**, *61*, 1022.
[34] Cisbio, "Human PD1/PD–L1 biochemical binding assay", can be found under https://www.cisbio.eu/human-pd1-pd-l1-biochemical-binding-assay-44666, **2020**.
[35] X. Lin, X. Lu, G. Luo, H. Xiang, *Eur. J. Med. Chem.* **2020**, *186*, 111876.
[36] B. Musielak, J. Kocik, L. Skalniak, K. Magiera-Mularz, D. Sala, M. Czub, M. Stec, M. Siedlar, T. A. Holak, J. Plewka, *Molecules* **2019**, *24*, 2804.
[37] A. Poschenrieder, M. Schottelius, M. Schwaiger, H. Kessler, H. J. Wester, *EJNMMI Res.* **2016**, *6*, 36.
[38] P. Antunes, M. Ginj, H. Zhang, B. Waser, R. P. Baum, J. C. Reubi, H. Maecke, *Eur. J. Nucl. Med. Mol. Imaging* **2007**, *34*, 982–993.
[39] J. C. Reubi, J. C. Schar, B. Waser, S. Wenger, A. Heppeler, J. S. Schmitt, H. R. Macke, *Eur. J. Nucl. Med.* **2000**, *27*, 273–282.
[40] C. Mejias, O. Guirola, *J. Mol. Graphics Modell.* **2019**, *91*, 105–111.
[41] H. Lim, J. Chun, X. Jin, J. Kim, J. Yoon, K. T. No, *Sci. Rep.* **2019**, *9*, 16727.
[42] C. A. Kluba, A. Bauman, I. E. Valverde, S. Vomstein, T. L. Mindt, *Org. Biomol. Chem.* **2012**, *10*, 7594–7602.
[43] N. M. Grob, S. Schmid, R. Schibli, M. Behe, T. L. Mindt, *J. Med. Chem.* **2020**, *63*, 4496–4505.

Manuscript received: February 17, 2022
Accepted manuscript online: April 7, 2022
Version of record online: April 28, 2022